Comparison of the H^+/ATP ratios of the H^+-ATP synthases from yeast and from chloroplast

Jan Petersen[a], Kathrin Förster[b], Paola Turina[c], and Peter Gräber[b,1]

[a]Department of Biochemistry and Molecular Biology, Monash University, Clayton, Victoria 3800, Australia; [b]Department of Physical Chemistry, University of Freiburg, D-79104 Freiburg, Germany; and [c]Laboratory of Biochemistry and Biophysics, Department of Biology, University of Bologna, I-40126 Bologna, Italy

Edited by Pierre A. Joliot, Institut de Biologie Physico-Chimique, Paris, France, and approved May 28, 2012 (received for review February 24, 2012)

F_0F_1-ATP synthases use the free energy derived from a transmembrane proton transport to synthesize ATP from ADP and inorganic phosphate. The number of protons translocated per ATP (H^+/ATP ratio) is an important parameter for the mechanism of the enzyme and for energy transduction in cells. Current models of rotational catalysis predict that the H^+/ATP ratio is identical to the stoichiometric ratio of c-subunits to β-subunits. We measured in parallel the H^+/ATP ratios at equilibrium of purified F_0F_1s from yeast mitochondria (c/β = 3.3) and from spinach chloroplasts (c/β = 4.7). The isolated enzymes were reconstituted into liposomes and, after energization of the proteoliposomes with acid–base transitions, the initial rates of ATP synthesis and hydrolysis were measured as a function of ΔpH. The equilibrium ΔpH was obtained by interpolation, and from its dependency on the stoichiometric ratio, [ATP]/([ADP]·[P_i]), finally the thermodynamic H^+/ATP ratios were obtained: 2.9 ± 0.2 for the mitochondrial enzyme and 3.9 ± 0.3 for the chloroplast enzyme. The data show that the thermodynamic H^+/ATP ratio depends on the stoichiometry of the c-subunit, although it is not identical to the c/β ratio.

chemiosmotic theory | protonmotive force | bioenergetics | nanomachine

Cells of all life kingdoms use H^+-ATP synthases to produce the cellular energy carrier ATP from the energy of a transmembrane electrochemical potential difference of protons built up and maintained by proton transport mechanisms, such as the oxidative electron transport in mitochondria or the photoinduced electron transport in chloroplasts (1). The number of protons translocated for each synthesized ATP molecule (H^+/ATP ratio) determines how large this difference of proton potential needs to be to maintain the high ATP/ADP ratio required by cell life. It is a key parameter in determining the flow of energy conversions in all living organisms. Ever since compelling experimental evidence in favor of a rotational mechanism for ATP synthases appeared (2–10), picturing them as molecular nanomachines in which two differently stepped motors (the membrane-embedded c-oligomer and the tripartite catalytic head) are connected by a central rotating shaft (γ/ε subunits), the general assumption has been that the H^+/ATP ratio should coincide with the ratio of the number of proton-binding c-subunits to the three catalytic nucleotide-binding β-subunits. Structural data have shown that the number of c-subunit monomers varies according to species (ref. 11 and references therein), with numbers that are mostly not multiples of three. Consequences of the above assumption are (*i*) the H^+/ATP ratio can vary among different species, and (*ii*) the H^+/ATP ratio can be a noninteger number. The number of β-subunits is three in all F_0F_1 analyzed so far, and the number of c-subunits varies between 8 and 15, resulting in predicted H^+/ATP ratios between 2.7 and 5.0. To our knowledge, neither of the two assumptions above has yet been experimentally challenged with the required accuracy.

In this work, we tested both assumptions by measuring in parallel the H^+/ATP ratio of the isolated and reconstituted H^+-ATP synthases from yeast mitochondria and from spinach chloroplasts. The c-subunit stoichiometry of the former is 10, as determined by X-ray crystallography of the whole complex (12, 13), and the stoichiometry of the latter is 14, according to X-ray crystallography (14, 15) and atomic force microscopy of the isolated c-ring (16). Hence, their respective H^+/ATP ratios, based on the assumptions mentioned above, should be 3.3 and 4.7. We have isolated the two complexes and reconstituted them into liposomes, which, if subjected to acid–base transitions to generate a high protonmotive force, were able to synthesize ATP at physiological rates (17, 18). The technique of acid–base transitions offers the great advantages of (*i*) measuring the imposed transmembrane ΔpH with the accuracy of the pH electrode, thus making high-precision quantitative studies possible (18–20), and (*ii*) allowing the testing of ATP synthases from different species with the same method and under identical experimental conditions.

Results

According to the chemiosmotic theory (1), the synthesis of ATP catalyzed by the H^+-ATP synthase is coupled to the translocation of $\boldsymbol{n}$ protons from the internal to the external compartment:

$$\mathrm{ADP} + P_i + \boldsymbol{n}H^+_{in} \leftrightarrow ATP + H_2O + \boldsymbol{n}H^+_{out}. \qquad [1]$$

The factor $\boldsymbol{n}$ is the number of protons translocated per ATP, and it is called the thermodynamic H^+/ATP ratio. The Gibbs free energy of this coupled reaction can be expressed as:

$$\begin{aligned}\Delta G' &= \Delta G'_p - \boldsymbol{n}\Delta\tilde{\mu}_{H^+} \\ &= \Delta G^{\circ\prime}_p + 2.3RT\log(Q) - \boldsymbol{n}(2.3RT\,\Delta pH + F\Delta\varphi),\end{aligned} \qquad [2]$$

where $\Delta\tilde{\mu}_{H^+}$ is the transmembrane electrochemical potential difference of protons, $\Delta G^{\circ\prime}_p$ is the Gibbs free energy of ATP synthesis, using the biochemical standard state, Q is the stoichiometric product: ([ATP]c^0)/([ADP][P_i]) with c^0 = 1 M, ΔpH is the transmembrane pH difference: $pH_{out} - pH_{in}$, Δφ is the transmembrane difference of electrical potential: $\varphi_{in} - \varphi_{out}$, and R, T, and F are gas constant, absolute temperature, and Faraday constant, respectively.

At the point of equilibrium ($\Delta G' = 0$), Eq. **2** becomes:

$$\begin{aligned}+2.3RT\log(Q) &= -\Delta G^{\circ\prime}_p + \boldsymbol{n}\Delta\tilde{\mu}_{H^+}(eq) \\ &= -\Delta G^{\circ\prime}_p + \boldsymbol{n}(2.3RT\,\Delta pH(eq) + F\Delta\varphi(eq)).\end{aligned} \qquad [3]$$

At constant Δφ(eq), only ΔpH(eq) and log(Q) are variables, and therefore, with a set of experimental values of log(Q) and

Author contributions: J.P., P.T., and P.G. designed research; J.P., K.F., and P.T. performed research; J.P., K.F., P.T., and P.G. analyzed data; and J.P., P.T., and P.G. wrote the paper.

The authors declare no conflict of interest.

This article is a PNAS Direct Submission.

Freely available online through the PNAS open access option.

[1]To whom correspondence should be addressed. E-mail: peter.graeber@physchem.uni-freiburg.de.

This article contains supporting information online at www.pnas.org/lookup/suppl/doi:10.1073/pnas.1202799109/-/DCSupplemental.

ΔpH(eq), both the H^+/ATP ratio $\boldsymbol{n}$ and $\Delta G^{\circ\prime}{}_p$ can be determined by linear regression analysis. In the present work, a constant Δφ of 60 mV (as evaluated from the Nernst equation) was applied to all measurements, to achieve higher rates of catalysis.

To apply this method we constructed a minimal chemiosmotic system (18, 19). Liposomes from phosphatidylcholine/phosphatidic acid were prepared, and either the chloroplast or the mitochondrial enzyme was reconstituted into the liposome membrane. When these proteoliposomes were energized by acid–base transitions they catalyzed rates of ATP synthesis up to 200 s^{-1} with CF_0F_1 (21, 22) and 100 s^{-1} with MF_0F_1 (17) (i.e., they displayed synthesis activities in the physiological range). Because for reconstitution of the enzymes the membrane was destabilized by addition of detergent (Triton X-100), it can be assumed that during this process (2 h) a full equilibration of all ion concentrations between the internal and external phases took place, so that the composition of the internal phase was known. Correspondingly, the pH_{in} value was taken to be identical to the pH of the reconstitution buffer, which was measured with a glass electrode after the reconstitution. The ion concentrations of the internal and external phases are collected in Table S1. The pH_{out} value resulted from the mixing of the acidic reconstitution buffer containing the proteoliposomes with the basic medium. At the mixing time ($t = 0$), a transmembrane ΔpH is established, which decays thereafter within a few minutes owing to passive and phosphorylating proton effluxes. Because pH_{in} and pH_{out} were measured with the same calibrated glass electrode, both parameters were known with high accuracy and precision, the error in the initial ΔpH measurement being smaller than 0.02 units (18). With the glass electrode the proton activities are detected, so that no further corrections were necessary for determination of ΔpH values.

To determine the ΔpH(eq) at each Q value (i.e., the ΔpH at which the phosphate potential is exactly balanced by ΔpH and the catalytic rate is zero), the initial rates of catalysis were measured at different initial ΔpHs at a constant stoichiometric product Q, so that both synthesis and hydrolysis could be observed, and the point of zero rate could be easily interpolated. The initial rates of catalysis were measured by rapid injection of the acidified proteoliposomes into the basic mixture, containing an ATP-monitoring luciferin/luciferase system. The ATP, ADP, and P_i concentrations in the basic medium were then varied within a wide range to establish different stoichiometric products Q (Table S2). In this way the initial rates of ATP synthesis and hydrolysis were measured both at different initial ΔpHs generated by the acid–base transition and at different Qs.

Typical measurements at $Q = 5.8$ and $pH_{out} = 8.38$ are shown in Fig. 1 for CF_0F_1 (*Upper Left*) and MF_1F_0 (*Upper Right*). Increase of luminescence indicates ATP synthesis, and decrease indicates ATP hydrolysis. The different curves refer to different initial ΔpH values as indicated. The initial rates were calculated by nonlinear regression analysis (*Materials and Methods*), and they are depicted in Fig. 1 as slopes at $t = 0$. The initial rates switched from ATP synthesis at the highest initial ΔpH to ATP hydrolysis at the lowest initial ΔpH. In each trace the rate of ATP synthesis decreased with time after the acid–base transition. In some traces (Fig. 1, *Upper Right*, trace at ΔpH = 1.68) the rate switched from ATP synthesis to ATP hydrolysis. This was because the measurements were carried out in the presence of both P_i/ADP and ATP, and therefore, as soon as the ΔpH had decreased below the thermodynamic threshold value of ΔpH(eq), the catalytic reaction switched from the synthesis to the hydrolysis direction. Additionally, the increase of the rate of ATP hydrolysis, observed in most hydrolysis traces, can be attributed to the decay of the initial ΔpH, and the corresponding release of its "backpressure" exerted on proton transport-coupled ATP hydrolysis. The initial rates of catalysis were calculated from the fitted traces and plotted against the initial ΔpH in Fig. 1, *Lower*.

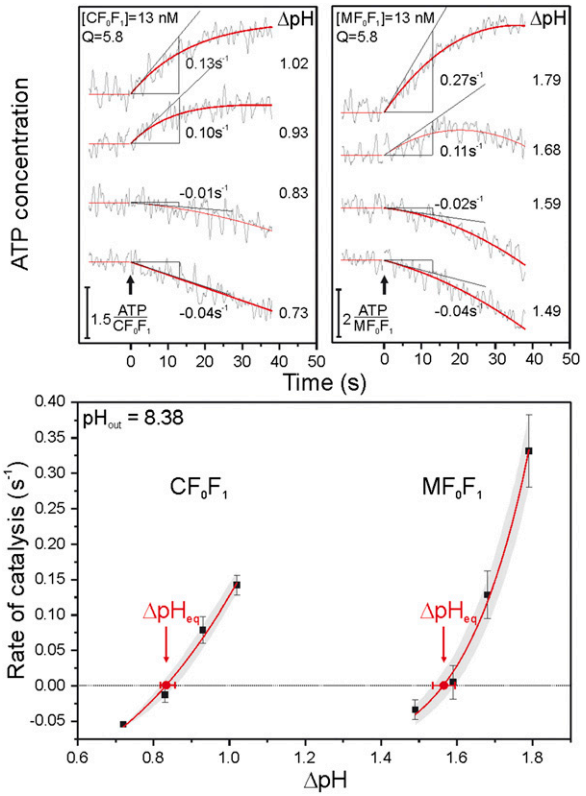

Fig. 1. ATP synthesis and hydrolysis after generation of different ΔpHs. *Upper*: Basic medium with luciferin/luciferase (720 μL) was placed in the luminometer, and the baseline was registered. Black arrows show the addition of the acidic proteoliposomes (80 μL) to the basic buffer. This addition gave rise to a shift of the baseline, which was shifted for clarity to the original luminescence level. The stoichiometric product Q = [ATP]/[ADP][P_i] was 5.8 ([ATP] = 596 nM, [ADP] = 10.3 μM), the pH_{out} was 8.38. Red solid lines are best fittings (see *Materials and Methods*) of the luminescence time trace; the initial rates were calculated from the fitted trace and shown as slopes at $t = 0$. The calibration of the ordinate is given in ATP per F_0F_1. *Upper Left*: Chloroplast enzyme, [CF_0F_1] = 13 nM; *Upper Right*: Mitochondrial enzyme, [MF_0F_1] = 13 nM. *Lower*: Initial rates of ATP synthesis (positive) and hydrolysis (negative) as a function of ΔpH. Each point is the average of three measurements, and black error bars are the corresponding SDs. The equilibrium ΔpHs [ΔpH(eq), red circles] were obtained by interpolation with a sigmoidal function. Red error bars of ΔpH(eq) resulted from the interpolation with the same function of the upper or lower error limits of the rates (shaded area).

The point of equilibrium ΔpH(eq) was obtained by interpolation to zero rate using a sigmoidal function. It was ΔpH(eq) = 0.84 ± 0.02 for CF_0F_1, and ΔpH(eq) = 1.57 ± 0.04 for MF_0F_1, with a difference of 0.73 ΔpH units between both enzymes at the same stoichiometric product ($Q = 5.8$). The error bars of ΔpH (eq) resulted from the interpolation with the same function of the upper and lower error limits of the rates (Fig. 1, *Lower*, shaded areas). The fitting with other functions (exponential or polynomial) yielded within error limits the same ΔpH(eq) values.

A correct interpolation requires that the same proton transport-coupled reaction is observed both in ATP synthesis and ATP hydrolysis direction. Whereas ATP synthesis is always coupled to proton transport, ATP hydrolysis can occur either coupled to proton transport or uncoupled from it. Uncoupled ATP hydrolysis might be catalyzed by reconstituted enzymes that are partially damaged and/or by nonreconstituted enzymes. When the ΔpH was abolished by addition of 10 μM nigericin, CF_0F_1 and MF_0F_1 showed different responses: CF_0F_1 did not show any ATP hydrolysis, whereas MF_0F_1 did. This is in agreement with previous results (18, 19) and confirms that CF_0F_1 is

a strongly regulated enzyme, which is inactive in the absence of a pre-energization by $\Delta\tilde{\mu}_{H^+}$ (23). We concluded that CF_0F_1 did not catalyze uncoupled ATP hydrolysis and that, therefore, no corrections for uncoupled ATP hydrolysis were required. For MF_0F_1 as well, the presence of a strong preactivation by $\Delta\tilde{\mu}_{H^+}$ has been reported (24). However, with MF_0F_1 small rates of ATP hydrolysis were detected in the presence of nigericin at Q values ≥1.87, and these rates increased with increasing Q value. The luciferin/luciferase technique detected changes of the ATP concentration in the medium, which resulted from the difference between ATP synthesis and coupled as well as uncoupled ATP hydrolysis. To calculate the rates of coupled ATP synthesis and hydrolysis from the change in ATP concentration, the rate of uncoupled ATP hydrolysis has to be determined. The two kinds of ATP hydrolysis can be distinguished by their different response to $\Delta\tilde{\mu}_{H^+}$. At high $\Delta\tilde{\mu}_{H^+}$, coupled ATP hydrolysis is completely inhibited, because proton pumping against a high protonmotive force is not possible, whereas uncoupled ATP hydrolysis is unaffected. The rate of ATP hydrolysis under high $\Delta\tilde{\mu}_{H^+}$ conditions (i.e., in the presence of a high rate of ATP synthesis) can be quantified with radioactive labeled ATP. The release of $^{32}P_i$ from [γ-^{32}P]ATP was measured in parallel in the absence and in the presence of a high $\Delta\tilde{\mu}_H$. Under the high $\Delta\tilde{\mu}_{H^+}$ conditions, any rate of hydrolysis would result only from the noncoupled enzymes, and this rate must be subtracted from the rate observed in the luciferin/luciferase assay to obtain the rate of the coupled catalysis.

Fig. 2, *Top*, shows the [γ-^{32}P]ATP hydrolysis at Q = 5.8 in the presence (filled circles) and absence (+nigericin, open circles) of a high $\Delta\tilde{\mu}_{H^+}$ (pH_{in} = 6.2, ΔpH = 2.1, $\Delta\varphi$ = 140 mV). The numbers at the slopes give the hydrolysis rates. When a higher $\Delta\tilde{\mu}_{H^+}$ (pH_{in} = 5.0, ΔpH = 3.3, $\Delta\varphi$= 140 mV) was used in the acid–base transition, the rates did not change, indicating that the maximal inhibition of the $\Delta\tilde{\mu}_{H^+}$-dependent hydrolysis rate had already been reached at ΔpH = 2.1, $\Delta\varphi$ = 140 mV. The rates obtained at the other Q values are reported in Fig. 2, *Middle* and Table S3. The rates measured at Q = 5.8 with the luciferin/luciferase assay (dotted line) and the same rates corrected for ATP hydrolysis by uncoupled enzymes (solid line) are shown in Fig. 2, *Bottom*. The $\Delta pH(eq)$ values before and after such correction were in this case 1.57 ± 0.04 and 1.53 ± 0.04, respectively. The corrections resulting for the $\Delta pH(eq)$s obtained at the other Q values are reported in Table S4.

Measurements of initial rates in the luciferin/luciferase assay at different ΔpHs were carried out at several constant Q values (Q = 0.1–16). These sets of initial rates, corrected as described above (Fig. 2, *Bottom*), are shown in Fig. 3 as a function of ΔpH for CF_0F_1 (*Upper*) and MF_0F_1 (*Lower*). All $\Delta pH(eq)$ values and the error limits were determined by interpolation as described in Fig. 1, and they ranged between 0.52 and 0.98 ΔpH units for CF_0F_1, and between 0.96 and 1.82 ΔpH units for MF_0F_1. As can be seen in Fig. 3, the dependencies of the rates on ΔpH were nonlinear, showing a slow rise in the ATP hydrolysis range and a steep rise in the ATP synthesis range. On the basis of the thermodynamics of irreversible processes, a linear relation between the rate and driving force (ΔpH) was expected. For CF_0F_1, this phenomenon has been analyzed (18): by correcting the observed nonlinear rate dependencies for the experimentally measured ΔpH dependency of enzyme preactivation, the expected linear relation was indeed obtained. This correction did not change, within error limits, the determined $\Delta pH(eq)$ values, because the sampling of ΔpH values was close enough to equilibrium compared with the curvature of the rate dependency. MF_0F_1 has been also shown to be preactivated by ΔpH (24), but no quantitative data are available. However, because the probed ΔpH values were similarly close to equilibrium, we concluded that no correction was needed for these data either. The dependencies of the rates on ΔpH showed different curvatures for the different Q values. Presumably, these differences can be attributed to regulatory effects of ADP and ΔpH. In particular, it can be observed that the curvature is generally less pronounced when, for a given ADP concentration, the $\Delta pH(eq)$ was increased owing to a higher ATP concentration. Regulatory phenomena, however, will not shift the point of thermodynamic equilibrium.

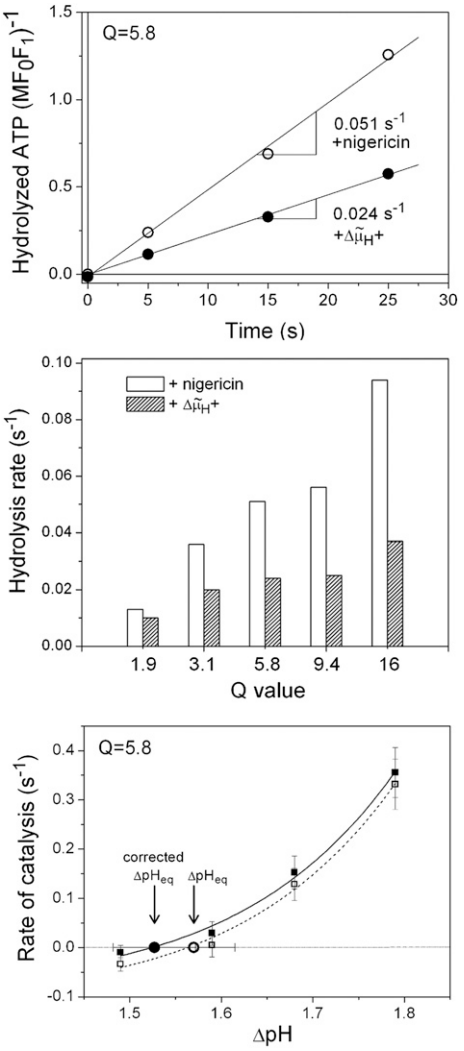

Fig. 2. Correction of the catalytic rates for the noncoupled rate of hydrolysis. *Top*: The $^{32}P_i$ released was measured at Q = 5.8 ([ATP] = 596 nM, [ADP] = 10.3 μM) as a function of time, as described in *Materials and Methods*. The acid–base transition was carried out at pH_{out} = 8.38 and pH_{in}= 6.3 and a K^+/valinomycin diffusion potential of 140 mV. Filled circles: the membrane was energized by the acid–base transition at time t = 0. Open circles: the acid–base transition was carried out as before, but the basic medium contained 10 μM nigericin to dissipate the $\Delta\tilde{\mu}_{H^+}$ generated across the membrane. The rates of ATP hydrolysis were determined by the slopes of the best-fitting straight lines. The errors in the determination of the slopes were below 4% and have been neglected. *Middle*: Rates of ATP hydrolysis at different stoichiometric ratios (nucleotide concentrations in Table S2) in the presence of 10 μM nigericin (open columns) or in the presence of $\Delta\tilde{\mu}_{H^+}$ (hatched columns). *Bottom*: Open circles: rate of ATP synthesis and ATP hydrolysis by MF_0F_1 as function of ΔpH. Data are from Fig. 1, *Lower*. The interpolating best-fitting curve (dashed line) and ΔpH (eq) are also shown. Solid circles: data obtained after correcting the rate measured with the luciferin/luciferase assay for ATP hydrolysis catalyzed by enzymes that were not coupled with proton transport. The $\Delta pH(eq)$ after correction is indicated by the solid circle.

The H^+/ATP ratio and $\Delta G^{\circ\prime}_p$ were determined from the dependence of $\Delta\tilde{\mu}_{H^+}(eq)$ on the preestablished stoichiometric

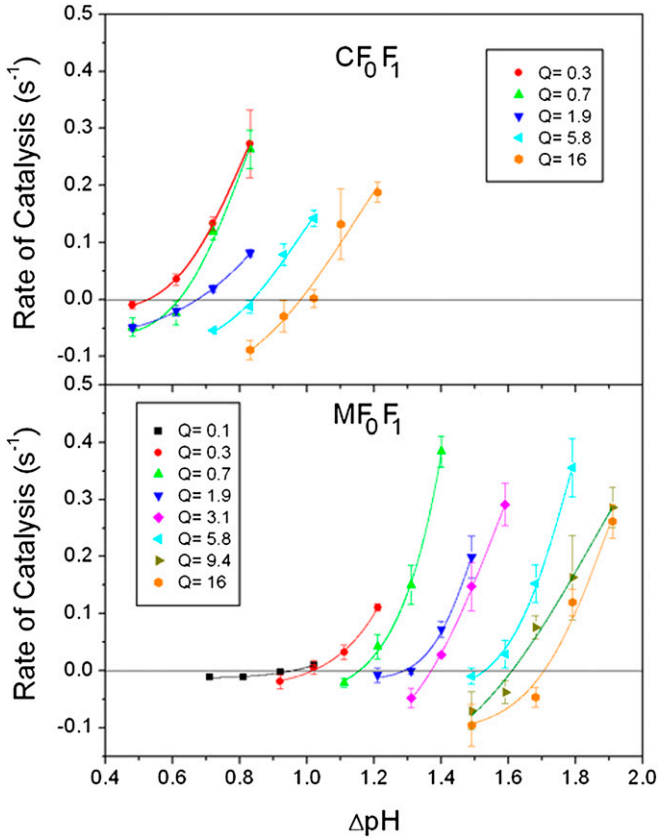

Fig. 3. Rates of catalysis as a function of ΔpH (in the presence of a constant Δφ). The rates of ATP synthesis and hydrolysis catalyzed by CF_0F_1 (*Upper*) and MF_0F_1 (*Lower*) are shown (at Δφ = 60 mV) as a function of ΔpH at different stoichiometric products. For MF_0F_1 with $Q \geq 1.9$, the initial rates were corrected for the hydrolysis rates that were not coupled with proton transport (Fig. 2). The equilibrium ΔpH for each curve was obtained by interpolation as described in Fig. 1. The different Q values were obtained by varying the ATP concentration from 50 to 750 nM and the ADP concentration from 51 to 4.6 μM at constant $[P_i]$ = 10 mM (Table S2).

product Q. The quantity 2.3RTlog(Q) and the corresponding transmembrane electrochemical potential difference of protons at equilibrium, $2.3RT\Delta pH(eq) + F\Delta\varphi(eq)$, were plotted in Fig. 4 for both CF_0F_1 (circles) and MF_0F_1 (triangles) and fitted by linear regression. According to Eq. **3**, the numerical values of the slopes give the thermodynamic H^+/ATP ratios $\boldsymbol{n}$: here, $\boldsymbol{n}$ = 3.9 ± 0.3 for CF_0F_1, and $\boldsymbol{n}$ = 2.9 ± 0.2 for MF_0F_1. In addition, the value of the y axis intercepts give the standard free energy of phosphorylation, $\Delta G^{\circ\prime}{}_p$, resulting in $\Delta G^{\circ\prime}{}_p$ = 37 ± 3 kJ·mol^{-1} for CF_0F_1 and $\Delta G^{\circ\prime}{}_p$ = 36 ± 3 kJ mol^{-1} for MF_0F_1. As expected, the same $\Delta G^{\circ\prime}{}_p$, within error limits, was obtained, because the same internal and external media were used for both enzymes.

Discussion

In this work, the H^+/ATP ratios of the yeast mitochondrial MF_0F_1 and of the chloroplast CF_0F_1 were measured in a simple chemiosmotic system, constituted by liposomes with the membrane-integrated enzymes. According to the chemiosmotic theory, the free energy of the chemical reaction (established by the imposed stoichiometric product Q) is balanced by the imposed electrochemical potential difference of protons $[\Delta\tilde{\mu}_{H^+}(eq)]$ multiplied by the stoichiometry $\boldsymbol{n}$ of the transported protons (the H^+/ATP ratio). The thermodynamics of the chemiosmotic theory does not require that the H^+/ATP ratio is an integer number; it is just the parameter necessary to adjust the energy balance.

The parallel measurement of H^+/ATP for both MF_0F_1 and CF_0F_1 under identical experimental conditions in this high-precision system ensured that the $\boldsymbol{n}$ values obtained for both enzymes can be directly compared, in particular the imposed $\Delta\tilde{\mu}_{H^+}$ values, the stoichiometric product Q, and the $\Delta G^{\circ\prime}{}_p$ were identical for both enzymes. Our results were H^+/ATP = 2.9 ± 0.2 for MF_0F_1 and H^+/ATP = 3.9 ± 0.3 for CF_0F_1. The CF_0F_1 value is in agreement with the value 4.0 (± 0.2) reported earlier (18, 19, 25, 26). As to MF_0F_1, different numbers, mainly 2 or 3, had been reported for the mammalian enzyme over the past decades (27, 28; for review see ref. 29), but no data had been published for the yeast MF_0F_1.

In the present measurements, the statistical errors in the values of the imposed parameters were small: the concentrations of nucleotides were preestablished and controlled spectroscopically, resulting in a vanishingly small error in the determination of the stoichiometric product Q. The error in the determination of the imposed ΔpH (at constant imposed Δφ) was minimized by using the same calibrated glass electrode for all measurements, and it has been estimated to amount to 0.02 pH units (18). The determination of ΔpH(eq) required an interpolation between the ATP synthesis and the ATP hydrolysis range, and possible systematic errors in this interpolation might have arisen. A correct interpolation requires that the same reaction (proton transport-coupled catalysis) is observed in both directions. No ATP hydrolysis was detected in CF_0F_1 in the absence of $\Delta\tilde{\mu}_{H^+}$, implying that the ATP hydrolysis measured in the energized CF_0F_1 proteolipomes was not due to damaged or nonreconstituted enzymes, but it resulted only from proton transport-coupled ATP hydrolysis. In MF_0F_1, ATP hydrolysis was detected also under deenergized conditions, implying that part of it could be uncoupled from the proton transport reaction. The method we have used to determine the fraction of the uncoupled reaction, and to correct for it, is based on the fact that a high $\Delta\tilde{\mu}_{H^+}$ will completely inhibit proton transport-coupled ATP hydrolysis, while not affecting any type of uncoupled ATP hydrolysis. This correction required the measurement of ATP hydrolysis by $^{32}P_i$ release, because this method allows the selective measurement of ATP hydrolysis in the presence of net ATP synthesis. The results of this procedure are shown in Fig. 2, and the corrected data are plotted in Fig. 4. To show the effect of this procedure on

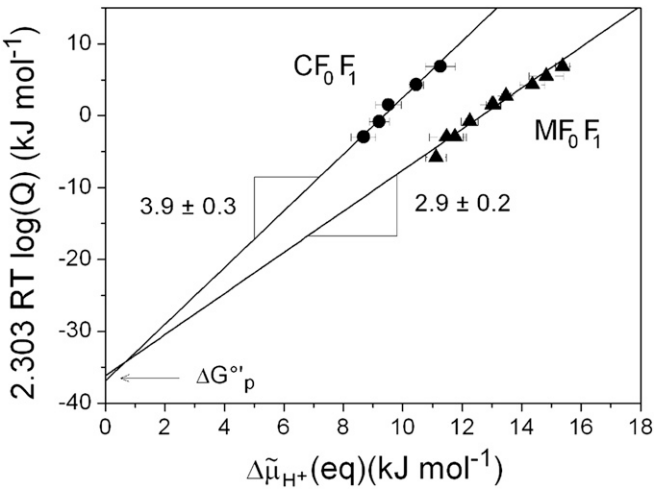

Fig. 4. Determination of the H^+/ATP ratio. Plot of the stoichiometric product 2.3RTlog(Q) vs. the electrochemical potential difference of protons at equilibrium $\Delta\tilde{\mu}_{H^+}$ (eq) (Eq. **3**) for CF_0F_1 (circles) and MF_0F_1 (triangles). The error bars indicate the error of ΔpH(eq) as described in the legend of Fig. 1. The slopes give the respective H^+/ATP ratios with SD. The intercepts at the ordinate axis give the standard free energy of ATP synthesis.

the final result, the data before and after correction were compared in Fig. S1 and Table S4. Without correction, $\boldsymbol{n} = 2.5 \pm 0.2$ and $\Delta G^{\circ\prime}_p = -32 \pm 3$ kJ/mol were obtained.

In addition to binding to catalytic sites, ATP might also bind to noncatalytic sites, and the luciferin/luciferase method does not distinguish between the two, because only changes in the free ATP in the medium are detected. ATP hydrolysis measured by $^{32}P_i$ release detects only the ATP that was bound to catalytic sites. In MF_0F_1, the rates of $^{32}P_i$ release measured in the absence of $\Delta\tilde{\mu}_{H^+}$ coincided, within error limits, with those measured in the absence of $\Delta\tilde{\mu}_{H^+}$ with the luciferin/luciferase assay, and from this result we concluded that ATP binding to noncatalytic sites could be excluded. In CF_0F_1, there was no detectable ATP binding to noncatalytic sites, as indicated by the constant ATP level measured in the absence of $\Delta\tilde{\mu}_{H^+}$ in the luciferin/luciferase assay. Both results are consistent with data on ATP binding to noncatalytic sites (see, e.g., refs. 30 and 31), indicating that the rate constants for ATP binding to those sites are at least two orders of magnitude smaller than those to catalytic sites.

The numerical value of the standard Gibbs free energy of ATP synthesis ($\Delta G^{\circ\prime}_p$) was not required by this method of $\boldsymbol{n}$ determination, because it resulted from the extrapolation of the 2.3RTlog(Q) dependency to $\Delta\tilde{\mu}_{H^+} = 0$ (Fig. 4). The same values of $\Delta G^{\circ\prime}_p$ were expected for both, MF_0F_1 and CF_0F_1, because all experimental conditions, except for the enzyme source, were identical. The fact that both CF_0F_1 and MF_0F_1 data sets resulted independently in the same $\Delta G^{\circ\prime}_p$, obtained by extrapolation over a wide $\Delta\tilde{\mu}_{H^+}$ range, constitutes an important piece of evidence for precision and internal consistency of the data. The numerical value is in accordance with that determined earlier (18, 19, 25) (obtained from coupling ATP synthesis/hydrolysis to the proton transport reaction) and also with those obtained from coupling the ATP hydrolysis with glutamine synthesis from glutamate and ammonia (32), or with acetate kinase and phosphate acetyl transferase (33).

In this work it is shown that H^+-ATP synthases isolated from different species can have different H^+/ATP ratios. That the H^+/ATP ratio differs among ATP synthases from different sources had been hypothesized (ref. 11 and references therein). As mentioned, a ratio of 4.0 (±0.2) for CF_0F_1 has been found previously (18, 19, 25, 26), and for the mammalian MF_0F_1, numbers varying from 2 to 3 have been reported (27–29). However, the key point of the present work is that the H^+/ATP ratios for yeast MF_0F_1 and CF_0F_1 have been determined in parallel under identical experimental conditions. This excludes the possibility that the different H^+/ATP ratios were due to different experimental conditions or methods.

High-resolution structural investigations have shown the presence of 14 c-subunits in the isolated c-ring of CF_0F_1 (14–16) and 10 c-subunits in the isolated yeast MF_0F_1 (12, 13). Our data indicate that the two H^+/ATP ratios correlate with the number of c-subunits in the two enzymes. If the c-subunit stoichiometry is the result of an evolutionary pressure, our data give support to the hypothesis (11, 28, 34) that this stoichiometry is one of the key energetic parameters nature can modulate according to the needs of different organisms.

Recently we have used the same method to compare the H^+/ATP ratios of the ATP synthases from *Escherichia coli* and from chloroplasts (19). We found that H^+/ATP = 4.0 ± 0.2 for CF_0F_1, in accordance with the present data, and H^+/ATP = 4.0 ± 0.3 for EF_0F_1. However, the c-subunit stoichiometry in EF_0 is not exactly known, because numbers between 12 (35) and 10 (36, 37) have been reported, and it has also been proposed to vary according to growth conditions (38). Therefore, for the *E. coli* enzyme, a meaningful comparison between the c/β ratio and the H^+/ATP ratio has to await further structural data.

Based on structural features, models of rotational coupling assume that (*i*) a 360° rotation of the γε-subcomplex produces three ATP molecules (one at each β-subunit), (*ii*) this rotation is coupled with a 360° rotation of the c_n-ring, and (*iii*) each c-subunit translocates one proton per rotation (39, 40). The H^+/ATP ratios predicted by these models are identical to the stoichiometric c/β ratios. With few exceptions (see, e.g., ref. 20) the number of c-subunits in the structures analyzed so far is not an integer multiple of three. Therefore, more recent models assume that the mismatch between the rotational steps in F_0 and those in F_1 is fully accommodated by the transient storage of the free energy of the protonation/deprotonation steps within the enzyme through elastic torsion mainly of the central stalk (refs. 11, 28, and 41 and references therein). The H^+/ATP ratio predicted by these models is identical to the stoichiometric c/β ratio, implying H^+/ATP = c/β= 14/3 = 4.7 for CF_0F_1 and H^+/ATP = c/β= 10/3 = 3.3 for the yeast MF_0F_1. The results of the present work show that the H^+/ATP ratios of 3.9 ± 0.3 for CF_0F_1 and 2.9 ± 0.2 for yeast MF_0F_1 correlate with but are outside error limits not identical to the predicted values of 4.7 and 3.3, respectively.

The difference between the H^+/ATP ratio measured in this work and the c/β ratio is surprising, and at the moment we can provide no reasonable explanation. However, the data support the idea that the number of c-subunits plays a major role in determining the H^+/ATP ratio. The finding that the thermodynamic H^+/ATP ratio can be significantly smaller than the c/β ratio indicates that the number of the energetically significant protons should not be automatically identified with the c/β ratio of the particular ATP synthase at issue.

Materials and Methods

Enzyme Isolation and Reconstitution. MF_0F_1 from *Saccharomyces cerevisiae* cells of the strain YRD15 was isolated as previously described (17). The MF_0F_1 complex was obtained in a buffer containing 20 mM Hepes/NaOH (pH 7.65), 250 mM sucrose, 1 mM EDTA, 4 mM $MgCl_2$, 5 mM 6-aminohexanoic acid, 1 mM DTT, 100 mM NaCl, and 1 mM dodecyl maltoside (Glycon), with a protein concentration of 5–10 μM, rapidly frozen, and stored in liquid nitrogen. CF_0F_1 was isolated from spinach chloroplasts (*Spinacia oleracea*) as previously described (18). The enzyme was obtained in a buffer containing 1.25 M sucrose, 30 mM NaH_2PO_4/NaOH (pH 7.2), 2 mM $MgCl_2$, 0.5 mM Na_2EDTA, and 4 mM dodecyl maltoside with a protein concentration of 7–10 μM, rapidly frozen in liquid nitrogen, and stored at −80 °C. The SDS/PAGE of a typical CF_0F_1 preparation is shown in Fig. S2. The nucleotides bound to the isolated complexes were determined by luciferin/luciferase ATP Kit (Roche) as described in ref. 42, resulting in 1.0 ± 0.1 ATP, 0.2 ± 0.1 ADP per MF_0F_1, and 1.1 ± 0.1 ATP, 1.0 ± 0.1 ADP per CF_0F_1. In control measurements, in which acid–base transitions were carried out in the absence of added ATP or ADP, the luciferin/luciferase signal remained constant in time, indicating that bound ATP was not released from the enzymes. Liposomes were prepared as follows: a dry lipid film was prepared by rotary evaporation of 10 mL chloroform containing 250 mg phosphatidylcholine and 12.5 mg phosphatidic acid, resuspended in 8 mL 10 mM Hepes (pH 7.6), 250 mM sucrose, 2 mM $MgCl_2$, and 1 mM EDTA and sonicated in 2-mL portions with a 3-mm-diameter tip for a total of 80 s (Branson Sonifier 250, step 2, 60% output), resulting in a lipid concentration of 32.8 mg/mL. MF_0F_1 or CF_0F_1 were reconstituted into the liposome membrane, similar to the method described earlier (17). To 150 μL reconstitution buffer (80 mM Mops, 80 mM Mes, 80 mM Hepes, 48 mM KCl, 40 mM NaH_2PO_4, and 70–240 mM NaOH), 150 μL liposomes, 40 μL protein solution (2 μM), 2.4 μL $MgCl_2$ (1 M), 52 μL Triton X-100 [10% (wt/vol)], and 206 μL H_2O were added to a final volume of 600 μL. The final enzyme concentration in this reconstitution mixture was 133 nM for both MF_0F_1 and CF_0F_1. Because of Triton X-100 treatment during reconstitution, the concentrations of all substances were equilibrated between the bulk phase and the internal proteoliposome phase; the resulting internal concentrations are collected in Table S1 and labeled as "Composition of internal phase." The reconstitution mixture was stirred slowly at room temperature for 30 min. Addition of 200 mg Biobeads led to the removal of Triton X-100 and the insertion of either MF_0F_1 or CF_0F_1 into the liposome membrane. The pH was measured with a glass electrode after reconstitution and is referred to as pH_{in}. The same buffers were used for reconstitution of MF_0F_1 and CF_0F_1, so that the internal pH had exactly the same value for both enzymes.

Measurement of Catalytic Activity. The ATP concentration was measured with a luciferin/luciferase ATP Kit (Roche) as described earlier (18, 19). All suspensions and solutions were equilibrated at room temperature (23 °C). Valinomycin was added to proteoliposomes to give a final concentration of 10 μM. A luminometer cuvette was filled with 20 μL of luciferin/luciferase kit; 700 μL of basic medium, containing 140 mM tricine, 143 mM KCl, 4 mM $MgCl_2$, 10.3 mM NaH_2PO_4, 98–100 mM NaOH, and different concentrations of ADP and ATP. The reaction was started by injection of 80 μL proteoliposomes into the cuvette placed in the luminometer (final volume, 800 μL). The pH value measured after this mixing was 8.38 ± 0.02, which was the pH of the external phase during the reaction (pH_{out}). The ion concentrations of the resulting external phase are summarized in Table S1. The final nucleotide concentrations ranged between 49 and 751 nM (ATP) and between 4.6 and 51.4 μM (ADP), and the final P_i concentration was 10 mM (Table S2). The nucleotide concentrations were determined spectroscopically as previously described (18). The final enzyme concentration in the reaction medium was 13.3 nM for both MF_0F_1 and CF_0F_1. The luminescence signal was calibrated by addition of a known amount of ATP. The luminescence data were sampled in 55-ms intervals. To determine the initial rates, the first 100–200 s of the signals were fitted with the sum of a monoexponential and a linear function (using the software package Origin), and the rates were calculated from the fitted function at $t = 0$.

The rates of ATP hydrolysis with superimposed high $\Delta\tilde{\mu}_{H^+}$ (ΔpH = 2.1, $[K^+]_{in}/[K^+]_{out}$ = 0.5/150 mM) were measured in the presence and in the absence of the uncoupler nigericin by the release of $^{32}P_i$ from [γ-^{32}P]ATP as previously described (43). These rates were used for correction of the catalytic rates obtained with the luciferin/luciferase system. Proteoliposomes were energized by an acid–base transition and an additional K^+/valinomycin diffusion potential in the presence of 10 mM P_i and various concentrations of ATP and ADP (Table S3) at room temperature (23 °C). Proteoliposomes (50 μL) were mixed with 50 μL of acidic medium and incubated for 3 min. Thereafter, the acid–base transition was carried out by adding 400 μL basic medium (±10 μM nigericin), which started the hydrolysis reaction, because it contained ADP and ATP at different concentrations and [γ-^{32}P]ATP (Hartmann Analytic) to a specific activity of 50–100 kBq/mL. Aliquots (100 μL) were withdrawn at 5, 15, and 25 s after the start of the reaction and mixed with 100 μL of 10% (wt/vol) trichloroacetic acid (TCA) for denaturation. The points at $t = 0$ were obtained by adding TCA (100 μL) to acidified proteoliposomes (10 μL proteoliposomes + 10 μL acidic medium), and then 80 μL of basic medium were added. The compositions of the internal and external phases were as reported in Table S1, except that the impermeant Mops, Mes, and Hepes buffers were replaced by 50 mM succinate, the internal KCl concentration was reduced to 0.5 mM, the internal pH was 6.2 (ΔpH = 2.1), and the enzyme concentration was 26 nM. The released $^{32}P_i$ was separated from [γ-^{32}P]ATP by organic solvent extraction of the molybdate–P_i complex, and the radioactivity was measured by liquid scintillation counting (43). The $^{32}P_i$ found at $t = 0$ amounted to approximately 2% of the total radioactivity and was subtracted from all data.

ACKNOWLEDGMENTS. We thank Mark Prescott and Rod Devenish for stimulating discussions.

1. Mitchell P (1966) Chemiosmotic coupling in oxidative and photosynthetic phosphorylation. *Biol Rev Camb Philos Soc* 41:445–502.
2. Boyer PD (1993) The binding change mechanism for ATP synthase—some probabilities and possibilities. *Biochim Biophys Acta* 1140:215–250.
3. Kinosita K, Jr., Adachi K, Itoh H (2004) Rotation of F_1-ATPase: How an ATP-driven molecular machine may work. *Annu Rev Biophys Biomol Struct* 33:245–268.
4. Abrahams JP, Leslie AG, Lutter R, Walker JE (1994) Structure at 2.8 A resolution of F_1-ATPase from bovine heart mitochondria. *Nature* 370:621–628.
5. Noji H, Yasuda R, Yoshida M, Kinosita K, Jr. (1997) Direct observation of the rotation of F_1-ATPase. *Nature* 386:299–302.
6. Sambongi Y, et al. (1999) Mechanical rotation of the c subunit oligomer in ATP synthase (F_0F_1): direct observation. *Science* 286:1722–1724.
7. Tsunoda SP, Aggeler R, Yoshida M, Capaldi RA (2001) Rotation of the c subunit oligomer in fully functional F1Fo ATP synthase. *Proc Natl Acad Sci USA* 98:898–902.
8. Junge W, et al. (2001) Inter-subunit rotation and elastic power transmission in F_0F_1-ATPase. *FEBS Lett* 504:152–160.
9. Diez M, et al. (2004) Proton-powered subunit rotation in single membrane-bound F_0F_1-ATP synthase. *Nat Struct Mol Biol* 11:135–141.
10. Zimmermann B, Diez M, Zarrabi N, Gräber P, Börsch M (2005) Movements of the ε-subunit during catalysis and activation in single membrane-bound H(+)-ATP synthase. *EMBO J* 24:2053–2063.
11. Watt IN, Montgomery MG, Runswick MJ, Leslie AG, Walker JE (2010) Bioenergetic cost of making an adenosine triphosphate molecule in animal mitochondria. *Proc Natl Acad Sci USA* 107:16823–16827.
12. Stock D, Leslie AG, Walker JE (1999) Molecular architecture of the rotary motor in ATP synthase. *Science* 286:1700–1705.
13. Dautant A, Velours J, Giraud MF (2010) Crystal structure of the Mg·ADP-inhibited state of the yeast F_1c10-ATP synthase. *J Biol Chem* 285:29502–29510.
14. Varco-Merth B, Fromme R, Wang M, Fromme P (2008) Crystallization of the c_{14}-rotor of the chloroplast ATP synthase reveals that it contains pigments. *Biochim Biophys Acta* 1777:605–612.
15. Vollmar M, Schlieper D, Winn M, Büchner C, Groth G (2009) Structure of the c_{14} rotor ring of the proton translocating chloroplast ATP synthase. *J Biol Chem* 284: 18228–18235.
16. Seelert H, et al. (2000) Structural biology. Proton-powered turbine of a plant motor. *Nature* 405:418–419.
17. Förster K, et al. (2010) Proton transport coupled ATP synthesis by the purified yeast H^+-ATP synthase in proteoliposomes. *Biochim Biophys Acta* 1797:1828–1837.
18. Turina P, Samoray D, Gräber P (2003) H^+/ATP ratio of proton transport-coupled ATP synthesis and hydrolysis catalysed by CF_0F_1-liposomes. *EMBO J* 22:418–426.
19. Steigmiller S, Turina P, Gräber P (2008) The thermodynamic H^+/ATP ratios of the H^+-ATPsynthases from chloroplasts and *Escherichia coli*. *Proc Natl Acad Sci USA* 105: 3745–3750.
20. Toei M, et al. (2007) Dodecamer rotor ring defines H^+/ATP ratio for ATP synthesis of prokaryotic V-ATPase from *Thermus thermophilus*. *Proc Natl Acad Sci USA* 104: 20256–20261.
21. Schmidt G, Gräber P (1985) The rate of ATP-synthesis by reconstituted CF_0F_1 liposomes. *Biochim Biophys Acta* 808:46–51.
22. Grotjohann I, Gräber P (2002) The H^+-ATPase from chloroplasts: effect of different reconstitution procedures on ATP synthesis activity and on phosphate dependence of ATP synthesis. *Biochim Biophys Acta* 1556:208–216.
23. Junesch U, Gräber P (1987) Influence of the redox state and the activation of the chloroplast ATP-synthase on proton-transport-coupled ATP-synthesis/hydrolysis. *Biochim Biophys Acta* 893:275–288.
24. Galkin MA, Vinogradov AD (1999) Energy-dependent transformation of the catalytic activities of the mitochondrial F0 x F1-ATP synthase. *FEBS Lett* 448:123–126.
25. Pänke O, Rumberg B (1997) Energy and entropy balance of ATPsynthesis. *Biochim Biophys Acta J* 1322:183–194.
26. Van Walraven HS, Strotmann H, Schwarz O, Rumberg B (1996) The H^+/ATP coupling ratio of the ATP synthase from thiol-modulated chloroplasts and two cyanobacterial strains is four. *FEBS Lett* 379:309–313.
27. Alexandre A, Reynafarje B, Lehninger AL (1978) Stoichiometry of vectorial H^+ movements coupled to electron transport and to ATP synthesis in mitochondria. *Proc Natl Acad Sci USA* 75:5296–5300.
28. Ferguson SJ (2000) ATP synthase: What dictates the size of a ring? *Curr Biol* 10: R804–R808.
29. Hinkle PC (2005) P/O ratios of mitochondrial oxidative phosphorylation. *Biochim Biophys Acta* 1706:1–11.
30. Kironde FA, Cross RL (1987) Adenine nucleotide binding sites on beef heart F1-ATPase. Asymmetry and subunit location. *J Biol Chem* 262:3488–3495.
31. Milgrom YM, Cross RL (1993) Nucleotide binding sites on beef heart mitochondrial F_1 ATPase. Cooperative interaction between sites e specificity of noncatalytic sites. *J Biol Chem* 268:23169–23175.
32. Rosing J, Slater EC (1972) Nucleotide-binding properties of native and cold-treated mitochondrial ATPase. *Biochim Biophys Acta* 267:275–290.
33. Guynn RW, Veech RL (1973) The equilibrium constants of the adenosine triphosphate hydrolysis and the adenosine triphosphate-citrate lyase reactions. *J Biol Chem* 248: 6966–6972.
34. Cross RL, Taiz L (1990) Gene duplication as a means for altering H^+/ATP ratios during the evolution of FoF1 ATPases and synthases. *FEBS Lett* 259:227–229.
35. Jones PC, Fillingame RH (1998) Genetic fusions of subunit c in the F_0 sector of H+-transporting ATP synthase. Functional dimers and trimers and determination of stoichiometry by cross-linking analysis. *J Biol Chem* 273:29701–29705.
36. Jiang W, Hermolin J, Fillingame RH (2001) The preferred stoichiometry of c subunits in the rotary motor sector of *Escherichia coli* ATP synthase is 10. *Proc Natl Acad Sci USA* 98:4966–4971.
37. Ballhausen B, Altendorf K, Deckers-Hebestreit G (2009) Constant c10 ring stoichiometry in the *Escherichia coli* ATP synthase analyzed by cross-linking. *J Bacteriol* 191: 2400–2404.
38. Tomashek JJ, Brusilow WS (2000) Stoichiometry of energy coupling by proton-translocating ATPases: A history of variability. *J Bioenerg Biomembr* 32:493–500.
39. Junge W, Lill H, Engelbrecht S (1997) ATP synthase: An electrochemical transducer with rotary mechanics. *Trends Biochem Sci* 22:419–423.
40. Vik SB, Antonio BJ (1994) A mechanism of proton translocation by F_1F_0 ATP synthases suggested by double mutants of the a subunit. *J Biol Chem* 269:30364–30369.
41. Junge W, Sielaff H, Engelbrecht S (2009) Torque generation and elastic power transmission in the rotary $F_{(O)}F_{(1)}$-ATPase. *Nature* 459:364–370.
42. Fromme P, Gräber P (1990) Activation/inactivation and uni-site catalysis by the reconstituted ATP-synthase from chloroplasts. *Biochim Biophys Acta* 1016:29–42.
43. Fischer S, Gräber P, Turina P (2000) The activity of the ATP synthase from *Escherichia coli* is regulated by the transmembrane proton motive force. *J Biol Chem* 275: 30157–30162.

Supporting Information

Petersen et al. 10.1073/pnas.1202799109

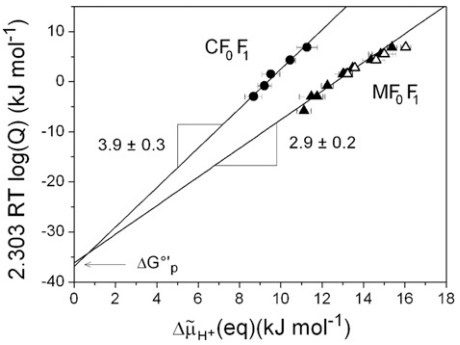

Fig. S1. Comparison between the MF_0F_1 data with and without correction for the noncoupled enzymes. Plot of 2.3RTlog(*Q*) vs. the electrochemical potential difference of protons at equilibrium $\Delta\tilde{\mu}_{H^+}(eq)$ for CF_0F_1 (circles), MF_0F_1 after correction for the $\Delta\tilde{\mu}_{H^+}$-independent hydrolysis (filled triangles), and MF_0F_1 data (open triangles) without correction for the $\Delta\tilde{\mu}_{H^+}$-independent hydrolysis. Data as in Fig. 4, plus the MF_0F_1 data (open triangles) without correction for the $\Delta\tilde{\mu}_{H^+}$-independent hydrolysis. Error bars indicate the error of ΔpH(eq) as described in the legend of Fig. 1. The slopes give the respective H^+/ATP ratios with SD. The intercepts at the ordinate axis give the standard free energy of ATP synthesis.

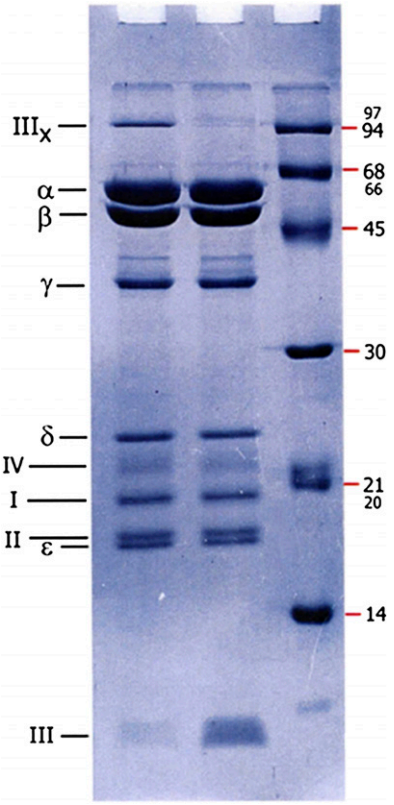

Fig. S2. SDS/PAGE of CF_0F_1 preparation. The CF_0F_1 samples were applied to a discontinuous 15% SDS/PAGE, which was stained with Coomassie Brilliant Blue. Left lane: CF_0F_1, after preparation; center lane: CF_0F_1, preincubated for 10 min at 95 °C; right lane: molecular weight standards. Subunits IV and III are homologous to subunits *a* and *c* of *Escherichia coli*, subunits I and II are both homologous to subunit *b* of *E. coli*. Heat treatment leads to dissociation of the subunit III complex (1).

1. Fromme P, Boekema EJ, Gräber P (1987) Isolation and characterization of a supramolecular complex of subunit III of the ATP-synthase from chloroplasts. *Z. Naturforsch* 42c:1239–1245.

Table S1. Composition of the proteoliposomes suspension before (internal phase) and after (external phase) the acid–base transitions

Reagent	Composition of internal phase	Composition of external phase
Mops (mM)	20	2.0
Mes (mM)	20	2.0
Hepes (mM)	20	2.0
NaOH (mM)	17 ÷ 51	88 ÷ 91
KCl (mM)	12	126
$MgCl_2$ (mM)	4.5	4
NaH_2PO_4 (mM)	10	10
Tricine (mM)	0	123
EDTA (mM)	0.25	0.025
Sucrose (mM)	63	6.3
DTT (mM)	0	5*
Valinomycin (μM)	—	10*
pH values	6.47 ÷ 7.77	8.38

The components from the storage media of the enzymes have been neglected. Such media were diluted 370- to 750-fold in the final assays. The MF_0F_1 complex was stored in a buffer containing 20 mM Hepes/NaOH (pH 7.65), 250 mM sucrose, 1 mM EDTA, 4 mM $MgCl_2$, 5 mM 6-aminohexanoic acid, 1 mM DTT, 100 mM NaCl, and 1 mM dodecyl maltoside, with a protein concentration of 5–10 μM. CF_0F_1 was obtained in a buffer containing 1.25 M sucrose, 30 mM NaH_2PO_4/NaOH (pH 7.2), 2 mM $MgCl_2$, 0.5 mM Na_2EDTA, and 4 mM dodecyl maltoside, with a protein concentration of 7–10 μM.

*DTT (50 mM, CF_0F_1 only) and 100 μM valinomycin were added to proteoliposomes 2 h before starting ATP synthesis/hydrolysis measurements.

Table S2. Nucleotide concentrations in the reaction medium and stoichiometric products, *Q*, for the different reaction conditions

ATP (μM)*	ADP (μM)	P_i (mM)	*Q*	log*Q*
0.049	51.4	10	0.095	−1.021
0.155	51.4	10	0.302	−0.520
0.369	51.4	10	0.718	−0.144
0.337	18.0	10	1.87	0.272
0.550	18.0	10	3.06	0.485
0.596	10.3	10	5.79	0.763
0.673	7.19	10	9.36	0.971
0.751	4.62	10	16.3	1.212

*These values include the amount of ATP present in the ADP solution (0.094% ATP of total ADP, as measured with the luciferin/luciferase assay).

Table S3. Hydrolysis rates at several *Q* values, measured by $^{32}P_i$-release, in the presence and absence of a maximal protonmotive force, as described in *Materials and Methods*

*Q**	Hydrolysis rate (s^{-1}) in the presence of 10 μM nigericin	Hydrolysis rate (s^{-1}) in the presence of protonmotive force
1.87	0.013	0.010
3.06	0.036	0.020
5.79	0.051	0.024
9.36	0.056	0.025
16.3	0.094	0.037

*ATP, ADP, and P_i concentrations as in Table S2.

Table S4. ΔpH(eq) values for MF_0F_1, determined before and after subtracting the hydrolysis rate, which was insensitive to the protonmotive force

Q	Hydrolysis rate (s^{-1}) in the presence of protonmotive force	Uncorrected ΔpH(eq)	Corrected ΔpH(eq)
0.095	ND	0.96 ± 0.03	0.96 ± 0.03
0.303	ND	1.02 ± 0.05	1.02 ± 0.05
0.303	ND	1.07 ± 0.03	1.07 ± 0.03
0.718	ND	1.15 ± 0.03	1.15 ± 0.03
1.87	0.010	1.32 ± 0.03	1.29 ± 0.03
1.87	0.010	1.33 ± 0.02	1.29 ± 0.02
3.06	0.020	1.39 ± 0.02	1.37 ± 0.02
5.79	0.024	1.57 ± 0.04	1.53 ± 0.04
9.36	0.025	1.64 ± 0.06	1.61 ± 0.06
16.3	0.037	1.82 ± 0.03	1.70 ± 0.03

ND, not determined.